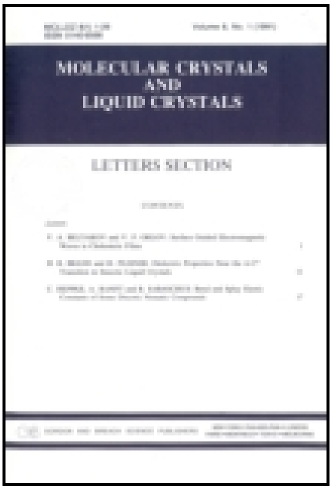

Molecular Crystals and Liquid Crystals
Publication details, including instructions for authors and subscription information:
http://www.tandfonline.com/loi/gmcl20

Solvent-Tolerant Patterning of Poly(3-hexylthiophene) Film by Subtractive Photolithography

Woo Young Kim[a], Won-Yong Lee[b], Gwang-Jae Jeon[c], Hyun-Bin Shim[c], In-Ku Kang[c], Jae-Hyun Kim[b], Gyung-Tae Park[b], Jin-Hyuk Kwon[b], Hee Chul Lee[c] & Jin-Hyuk Bae[b]

[a] Department of Mechanical Engineering, Korea Advanced Institute of Science, and Technology, Yuseong-Gu, Daejeon, Republic of Korea

[b] School of Electronics Engineering, Kyungpook National University, Bukgu, Daegu, Republic of Korea

[c] Department of Electrical Engineering, Korea Advanced Institute of Science, and Technology, Yuseong-Gu, Daejeon, Republic of Korea
Published online: 17 Nov 2014.

Mol. Cryst. Liq. Cryst., Vol. 599: pp. 36–42, 2014

ISSN: 1542-1406 print/1563-5287 online
DOI: 10.1080/15421406.2014.935917

Taylor & Francis
Taylor & Francis Group

Solvent-Tolerant Patterning of Poly(3-hexylthiophene) Film by Subtractive Photolithography

WOO YOUNG KIM,[1,†] WON-YONG LEE,[2,†] GWANG-JAE JEON,[3] HYUN-BIN SHIM,[3] IN-KU KANG,[3] JAE-HYUN KIM,[2] GYUNG-TAE PARK,[2] JIN-HYUK KWON,[2] HEE CHUL LEE,[3] AND JIN-HYUK BAE[2,*]

[1]Department of Mechanical Engineering, Korea Advanced Institute of Science, and Technology, Yuseong-Gu, Daejeon, Republic of Korea
[2]School of Electronics Engineering, Kyungpook National University, Bukgu, Daegu, Republic of Korea
[3]Department of Electrical Engineering, Korea Advanced Institute of Science, and Technology, Yuseong-Gu, Daejeon, Republic of Korea

This study investigates how the fringing field affects the total current flow within a conducting polymer. In order to extract the fringing field component of bar pattern resistors, a solvent-assisted patterning method using subtractive photolithography was successfully established for the conducting polymer poly(3-hexylthiophene). By comparing the current quantities of unpatterned and patterned resistors, a conductance factor for the fringing field was calculated, proving to be almost constant regardless of the resistor length. It is therefore concluded that the length as well as the width of the conducting polymer film need to be suitably patterned for the precise operation of organic electronic devices. In this regard, the patterning method developed will be useful for the fabrication of micro-scale devices.

Keywords poly(3-hexylthiophene); P3HT; photolithography; lift-off; fringing field

Introduction

Recently, newly emerging systems based on organic materials have been the subject of research into their potential use in flexible displays, transparent devices, and large-area devices [1–3]. The challenges posed by such applications are based on obtaining organic materials with special characteristics, like mechanical flexibility and optical transparency

---

†These authors contributed equally to this work.

*Address correspondence to Prof. Jin-Hyuk Bae, School of Electronics Engineering, Kyungpook National University, 1370 Sankyuk-dong, Bukgu, Daegu, 702-701, Republic of Korea. Tel.: +82-53-950-7222; Fax: +82-53-950-7222. E-mail: jhbae@ee.knu.ac.kr

Color versions of one or more of the figures in the article can be found online at www.tandfonline.com/gmcl.

in the visible light range. Moreover, these organic materials also have roll-to-roll process compatibility, such as is required for screen-printing and ink-jet processes [4–7]. However sophisticated they may be, these organic electronic devices also require fine patterning technology to produce high performance integrated system as silicon integrated circuits (ICs) that exhibit high-speed, low-power consumption, and interference-resistance operation. High-speed operation requires a narrower channel length in transistors, and low-power consumption can be achieved by blocking leakage current paths. In large-scale ICs, electromagnetic interference or coupling can occur among metal/high-k dielectric/metal components. A number of processing steps must therefore be included in patterning in order to achieve these issues. Though many patterning methods have been suggested so far, there is no direct replacement for photolithography among them [8]. Thus, at present, photolithography remains the only process suitable for reproducible and fine patterning in mass-production.

Photolithography of conducting polymers using a dry etching process has already has been reported [9]. In this, the necessity of dry etching over wet was emphasized because of the severe undercut in comparison to the organic layer that occurs below the photoresist layer that occurs in the case of wet etching. However, in spite of the fine patterns obtained with dry etching, it is expected that the oxygen radicals produced during this process may disrupt the underlying organic films through material degradation and undesired substrate etching. Such side effects can be avoided if a wet etching process can be established, and a vacuum-free process will help reduce the total process time and enable much larger-area systems to be manufactured.

In this paper, a solvent-assisted patterning technology for conducting polymers is demonstrated, which is based on photolithography. In order to ensure precise and fine patterns, a lift-off process has been adopted. In addition, the fringing field component of the conducting polymer is extracted by subtraction of two current components, in the form of both a patterned and unpatterned bar resistor. Finally, micro-scale patterns are used to prove the effectiveness of the newly developed solvent-assisted patterning method.

Experimental

For the conducting polymer, regioregular poly(3-hexylthiophene), or rr-P3HT, was purchased from Solaris Chem. To purify and remove any residual metal catalysts from its synthesis, a Soxhlet extraction process was performed as previous studies [10]. A 0.01 g sample of rr-P3HT was dissolved in 1 mL of mono-chlorobenzene by stirring for 24 hours, and the solution was then filtered. For spin coating under conditions of 1500 rpm and 10 s, the thickness of the rr-P3HT used was 40 nm. In order to ensure solubility, rr-P3HT films were first dipped into the different solvents typically used during photolithography. In the cases of acetone (used as a photoresist stripper), n-methyl pyrrolidone (NMP, also used as a photoresist stripper), tetra-methyl ammonium hydroxide (TMAH, used as a photoresist developer), and propylene glycol monomethyl ether acetate (PGMEA, used as a photoresist solvent), the rr-P3HT films did not dissolve; which is consistent with previously reported results [9, 12].

A commercialized negative photoresist, AZ2035, was spin-coated (thickness = 2.5 mm) and pattered by *i*-line (365 nm) onto a SiO_2/Si wafer that had been prepared by cleaning with piranha solution (mixture of H_2SO_4 and H_2O_2). The rr-P3HT solution was then spin-coated onto this patterned photoresist layer. After drying at 100°C for 10 min, the AZ2035 was removed using a commercial photoresist stripper, AZ400T.

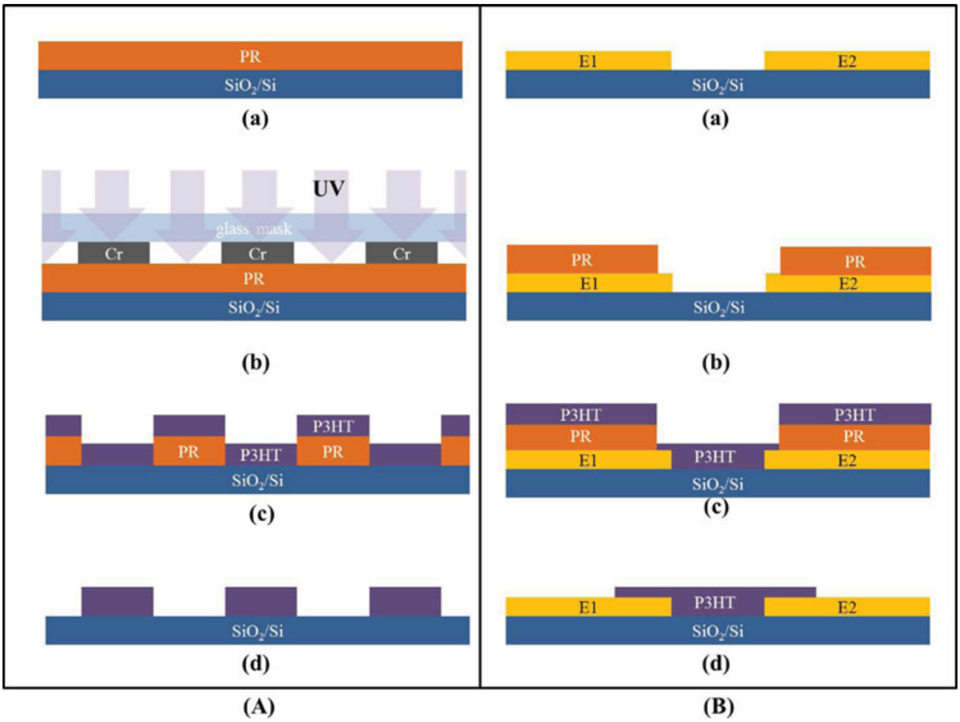

Figure 1. The process flow chart for (A) rr-P3HT patterning, and (B) rr-P3HT resistor fabrication.

Bar type resistors were fabricated as follows: First, two electrodes were deposited through a shadow mask on a SiO_2/Si wafer (Cr/Au = 10 nm / 100 nm). The lengths (L) between the two electrodes were varied as 50, 80, 130, 180, and 230 μm; and all widths (W) were identical at 1000 μm. The current-voltage characteristics were measured with a HP4156 parameter analyzer. A flow chart depicting all these processes is depicted in Fig. 1.

Results and Discussion

Figure 2 shows optical microscopy images of (A) an unpatterned resistor and (B) a patterned resistor. To clarify the current paths, these are depicted by arrows in the schematics (SA) and (SB). For the unpatterned resistor, when a voltage (V_2) is applied the current will flow between the two electrodes, E1 and E2, through three different paths: the shortest path (i(R)); and two side paths, $i(R_{F1})$ and $i(R_{F2})$, that arise as a result of the fringing field. The total current (i_2) is therefore simply determined by the sum of i(R), $i(R_{F1})$ and $i(R_{F2})$:

$$\begin{aligned} i_2 &= i(R) + i(R_{F1}) + i(R_{F2}) = \frac{V_2}{R} + \frac{V_2}{R_{F1}} + \frac{V_2}{R_{F2}} \\ &= (G + G_{F1} + G_{F2})V_2 \end{aligned} \tag{1}$$

Where R is the resistance of the patterned region in Fig. 2 (SB), and R_{F1} and R_{F2} are the respective resistances of the two side paths. G, G_{F1} and G_{F2} are the conductance values for R, R_{F1} and R_{F2}, respectively. When V_1 is applied to a patterned resistor, the total current (i_1) is expressed as GV_1. If it is assumed that $V = V_1 = V_2$, and by subtracting i_1 from i_2,

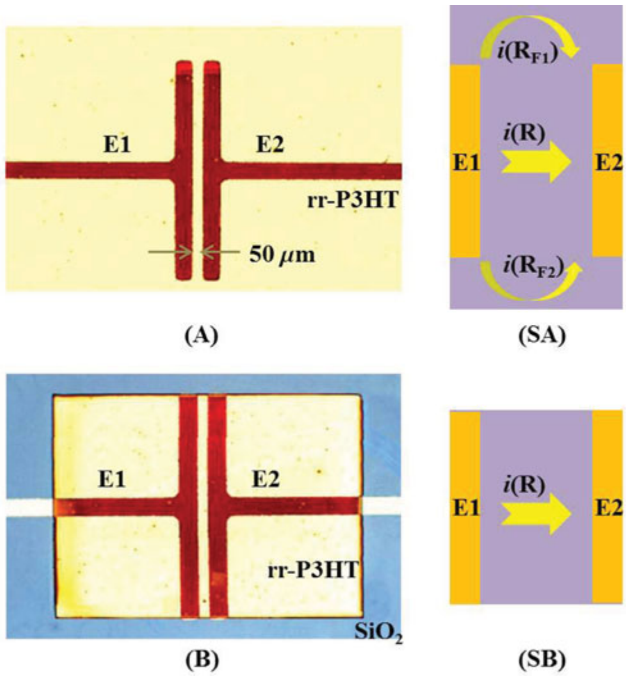

Figure 2. Optical microscopy images of (A) unpatterned resistor, and (B) patterned resistor; where $L = 50$ μm, and (SA) and (SB) are schematics of the current paths of unpatterned and patterned resistors, respectively.

the conductance of the fringing field can be determined as follows:

$$G_F = \frac{i_2 - i_1}{V} \tag{2}$$

where G_F is the sum of G_{F1} and G_{F2}. From equation (2), the parasitic conductance induced by the fringing field is extracted directly for the specific applied voltage, V.

One condition that must be checked in adapting the aforementioned equations is that the contact of the two materials (rr-P3HT and Au) is ohmic. Figure 3 shows the current-voltage characteristics, and from the linearity of Fig. 3(A) it is clear that the rr-P3HT-Au contacts are ohmic for both unpatterned and patterned resistors. It should also be noted that the current for each of the different lengths was measured at a constant voltage of 10 V. In Fig. 3(B), all of the unpatterned resistors show a greater current flow than the patterned resistors. Specifically, the unpatterned resistors exhibit current values that vary from 0.34 μA at $L = 50$ μm to 0.14 μA at $L = 230$ μm; whereas with patterned resistors the current varies from 0.24 μA at $L = 50$ μm to 0.03 μA at $L = 230$ μm. Furthermore, the contact resistance (for $L = 0$) of the patterned resistors is ~33.7 MΩ. Therefore, the conductance (G) of rr-P3HT itself is 0.125 μS for $L = 50$ μm, which is similar to previously reported values [13]. The conductivity is calculated as 1.56 mS/cm.

From equation (2), the fringing field components (G_F) were calculated as 9 nS in Fig. 3(C). Interestingly, there appears to be no relationship between L and G_F, which has two important meanings: First, is that the fringing field effect cannot be avoided unless the

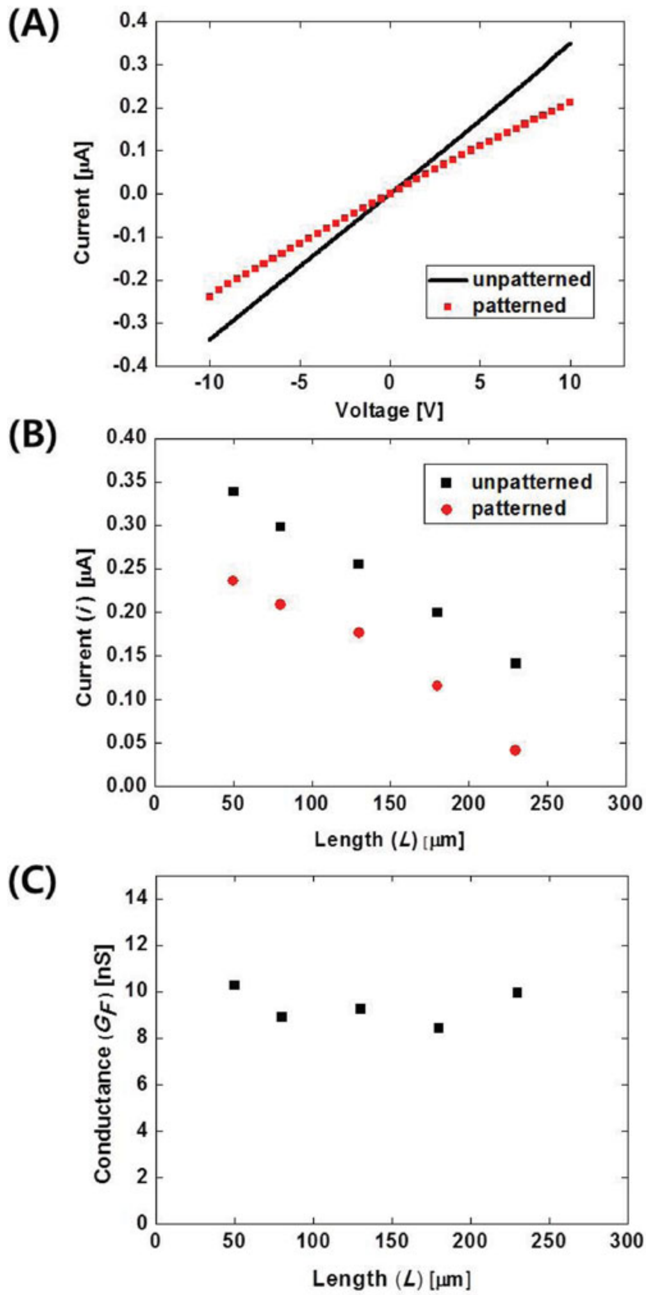

Figure 3. The current-voltage characteristics, (A) current-voltage relationships for $L = 50\ \mu$m, (B) current-resistor length relationship for $V = 10$ V, and (C) conductance, G_F, by fringing field.

conducting layer is patterned; and thus a very fine electrode patterning (small L) is not sufficient for high performance. In other words, two-dimensional patterns are the most meaningful for high performance devices. Second, organic field effect transistors strongly require an active layer patterning. Normally, the channel length reduction for scaling has

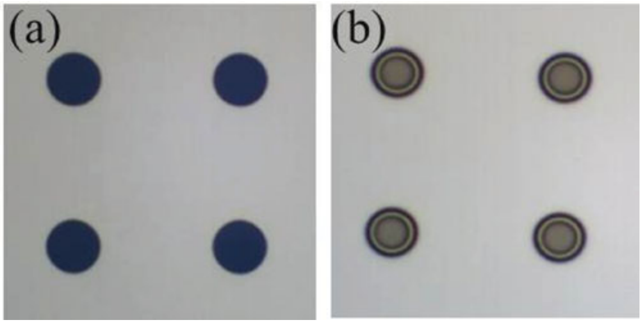

Figure 4. Optical microscopy images of (a) mask pattern, and (b) patterned P3HT. All have a diameter of 15 μm.

been utilized for patterning; however, from these results for the fringing field effect, it is clear that the channel width must also be considered.

The usefulness of the lift-off process for fine patterning is demonstrated by the two optical microscopy images shown in Fig. 4. In this, the left image depicts the Cr-mask patterns, which have a diameter of 15 μm. For the patterned rr-P3HT, the right image shows a circular array almost identical in size, which contradicts the findings of a previous report [9]. In other words, a wet etching process can also produce a fine and reproducible pattern. The previous report also demonstrated that wet-etching patterning suffers limitations caused by a severe undercut phenomenon [9]. However, in this work, 15 μm-sized circles were successfully patterned as a mask. If more precise exposure systems are permitted, then finer patterns will undoubtedly be formed.

Conclusion

In conclusion, the solvent-assisted patterning of an organic conducting film was successfully demonstrated by means of photolithography and a lift-off process, which enables an identically-sized pattern to be transferred from a mask to the rr-P3HT film. Through a comparison of patterned and unpatterned rr-P3HT resistors, it was found that the fringing effect is not dependent on variations in the resistor length. Thus, the width as well as the length of a conducting film must be taken into consideration for patterning. Using this newly developed solvent-assisted lithographic patterning technique, micro-scale organic devices can be fabricated. This patterning method will therefore be useful for the development of high performance organic devices.

Acknowledgments

The authors wish to acknowledge the assistance provided by Solaris Chem. in performing the Soxhlet extraction to purify the organic material. This work was also supported by the Preparatory Project (N10110074); the Brain Korea 21 Project, BK Electronics and Communications Technology Division, KAIST, in 2012; and the Basic Science Research Program through the National Research Foundation of Korea (NRF), funded by the Ministry of Education (2013R1A1A4A01009807).

References

[1] [online] http://www.oled-info.com/flexible-oled
[2] Yang, Y., Jeong, S., Hu, L., Wu, H., Lee, S. W., & Cui, Y. (2011). *Proc. Natl. Acad. Sci.*, *108*, 13013.
[3] Someya, T., Sekitani, T., Iba, S., Kato, Y., Kawaguchi,and, H., & Sakurai, T. (2004). *Proc. Natl. Acad. Sci.*, *101*, 9966.
[4] Berggren, M., Nilsson, D., & Robinson, N. D. (2007). *Nat. Mater.*, *6*, 3.
[5] Bao, Z. N., Feng, Y., Dodabalapur, A., Raju, V. R., & Lovinger, A. J. (1997). *Chem. Mater.*, *9*, 1299.
[6] Chang, S. C., Bharathan, J., Yang, Y., Helgeson, R., Wudl, F., Ramey, M. B., & Reynolds, J. R. (1998). *Appl. Phys. Lett.*, *73*, 2561.
[7] Hebner, R., Wu, C. C., Marcy, D., Lu, M. H., & Sturm, J. C. (1998) *Appl. Phys. Lett.*, *72*, 519.
[8] Taylor, P. G., Lee, J.-K., Zakhidov, A. A., Chatzichristidi, M., Fong, H. H., DeFranco, J. A., Malliaras, G. G., & Ober, C. K. (2009). *Adv. Mater.*, *21*, 2314.
[9] Balocco, C., Majewski, L. A., & Song, A. M. (2006). *Org. Electron*, *7*, 500.
[10] Naber, R. C. G., de Boer, B., Blom, P. W. M., & de Leeuw, D. M. (2005). *Appl. Phys. Lett.*, *87*, 203509.
[11] Material Safety Data Sheet of AZ400T.
[12] Material Safety Data Sheet of AZ2035.
[13] Naber, R. C. G., Mulder, M., de Boer, B., Blom, P. W. M., & de Leeuw, D. M. (2006). *Org. Electron*, *7*, 132.